Adenovirus-expressed human hyperplasia suppressor gene induces apoptosis in cancer cells

Lina Wu,[1] Zhixin Li,[1] Yingmei Zhang,[1] Pei Zhang,[1] Xiaohui Zhu,[1] Jing Huang,[1] Teng Ma,[1] Tian Lu,[1] Quansheng Song,[1] Qian Li,[2] Yanhong Guo,[2] Jian Tang,[2] Dalong Ma,[1] Kuang-Hueih Chen,[2] and Xiaoyan Qiu[1]

[1]Center for Human Disease Genomics, Health Science Center and [2]Institute of Cardiovascular Science and Institute of Molecular Medicine, Peking University, Beijing, China

Abstract

Hyperplasia suppressor gene (HSG), also called human mitofusin 2, is a novel gene that markedly suppresses the cell proliferation of hyperproliferative vascular smooth muscle cells from spontaneously hypertensive rat arteries. This gene encodes a mitochondrial membrane protein that participates in mitochondrial fusion and contributes to the maintenance and operation of the mitochondrial network. In this report, we showed that an adenovirus vector encoding human HSG (Ad5-hHSG) had an antitumor activity in a wide range of cancer cell lines. We further focused on the lung cancer cell line A549 and the colon cancer cell line HT-29 and then observed that Ad5-hHSG induced apoptosis both *in vitro* and *in vivo*. Confocal laser scanning microscopy and electron microscopy revealed that cells infected with Ad5-hHSG formed dose-dependent perinuclear clusters of fused mitochondria. Adenovirus-mediated hHSG overexpression induced apoptosis, cell cycle arrest, mitochondrial membrane potential ($\Delta\Psi$m) reduction and release of cytochrome *c*, caspase-3 activation, and cleavage of PARP *in vitro*. Overexpression of hHSG also significantly suppressed the growth of subcutaneous tumors in nude mice both *ex vivo* and *in vivo*. In addition, Ad5-hHSG increased the sensitivity of these cell lines to two chemotherapeutic agents, VP16 and CHX, and radiation. These results suggest that Ad5-hHSG may serve as an effective therapeutic drug against tumors. [Mol Cancer Ther 2008;7(1):222–32]

Introduction

Hyperplasia suppressor gene (HSG) is a novel gene characterized by Chen et al. as a cell proliferation suppressor (1). It was originally named hypertension-related gene-1 because it was found in cultured vascular smooth muscle cells of Wistar-Kyoto and spontaneous hypertension rats using mRNA differential display technology (2). The expression of hypertension-related gene-1 mRNA was lower in spontaneous hypertension rat than Wistar-Kyoto rat. Moreover, vascular smooth muscle cell proliferation was inhibited by hypertension-related gene-1 (3). The hypertension-related gene-1 name was changed to HSG after overexpression was found to suppress serum-evoked vascular smooth muscle cell proliferation in culture. Because rHSG shares 95.2% and 98.4% similarity with its human and mouse homologues, respectively, we cloned human HSG (hHSG) to further explore its function. hHSG is located in chromosome 1p36.3. hHSG is also named human mitofusin 2 (Mfn2), because its homologue, Mfn1, plays a vital role in mitochondrial fusion by regulating mitochondrial morphology and function in mammalian cells, yeast, and flies (4–7). When transiently expressed in mammalian cells, both variants, Mfn1 and Mfn2, induce formation of highly elongated and interconnected mitochondrial tubules. Recent studies have indicated that Bax or Bak is required for normal fusion of mitochondria into elongated tubules. Bax induces mitochondrial fusion by activating assembly of the large GTPase Mfn2 through interaction with coiled-coil domain of Mfn2 (8). As a proapoptosis protein, Bax colocalizes with Mfn2 during apoptosis (9). These evidences imply that hHSG may be also involved in apoptosis.

In this study, to investigate hHSG bioactivity, we constructed an adenovirus expression vector of hHSG (Ad5-hHSG) and found that Ad5-hHSG had a wide antitumor effect *in vitro*. Interestingly, it was not efficient in some diploid cell lines. *In vitro* and *in vivo* experimental data confirmed that hHSG overexpression induces cancer cell apoptosis, along with mitochondrial membrane potential ($\Delta\Psi$m) reduction and release of cytochrome *c*. In addition, Ad5-hHSG also induced chemosensitization and radiosensitization of A549 and HT-29 cells. Our results suggest that adenovirus-mediated hHSG gene transfer may present a new therapeutic approach for cancer treatment.

Received 6/8/07; revised 10/1/07; accepted 12/3/07.

Grant support: National High Technology Research and Development Program of China grant 2002AA216131.

The costs of publication of this article were defrayed in part by the payment of page charges. This article must therefore be hereby marked *advertisement* in accordance with 18 U.S.C. Section 1734 solely to indicate this fact.

Note: L. Wu and Z. Li contributed equally to this work.

Present address for Zhixin Li: Department of Integrated Traditional Chinese Medicine and Western Medicine, Health Science Center, Peking University, 38 Xue-yuan Road, Beijing, 100083, P.R. China.

Requests for reprints: Xiaoyan Qiu, Center for Human Disease Genomics, Health Science Center, Peking University, 38 Xue-yuan Road, Beijing, 100083, P.R. China. Phone: 86-10-82802846-5035. Fax: 86-10-82801149. E-mail: qiuxy@bjmu.edu.cn or Kuang-Hueih Chen. E-mail: ChenKu@grc.nia.nih.gov

doi:10.1158/1535-7163.MCT-07-0382

Materials and Methods

Cell Lines and Cell Culture

A549, HeLa, HT-29, MCF-7, HEK293, normal human foreskin fibroblast cell line BJ, HL-60, K562, Raji, and U937 were obtained from American Type Culture Collection. Normal liver cell line L02 was obtained from the cell bank of Type Culture Collection of Chinese Academy of Science.

A549, HeLa, HT-29, MCF-7, L02, and HEK293 were cultured in DMEM (Life Technologies) supplemented with 10% fetal bovine serum (Hyclone), 2 mmol/L glutamine, 100 units/mL penicillin, and 100 μg/mL streptomycin. BJ was cultured in MEM medium (Life Technologies) supplemented as above. HL-60, K562, Raji, and U937 were cultured in RPMI 1640 (Life Technologies) supplemented as above. All the cells were maintained in an incubator with a humidified atmosphere of 95% air and 5% CO_2 at 37°C.

Construction and Purification of Ad5-hHSG

The complete coding region hHSG PCR product was subcloned into the pDC316-cytomegalovirus shuttle vector. The pDC316-hHSG DNA was recombined with backbone pAdEasy-1 in BJ5183 bacteria. Adenovirus generation, amplification, and titer were done according to the simplified system described by He et al. (10). Viral particles were purified by cesium chloride density gradient centrifugation. The control virus or the virus containing hHSG was named Ad5-Null or Ad5-hHSG, respectively.

Cell Viability Assay

Cell viability after infection with different adenoviral vectors was determined using the Vi-CELL TMXR cell viability analyzer (Beckman Coulter). Trypan blue–positive cells were considered dead, and the numbers of viable cells were calculated by the analyzer according to the manufacturer's instructions.

Reverse Transcription – PCR Analysis

Detection of hHSG mRNA expression was carried out by reverse transcription–PCR. Cells were collected at indicated time points, and RNA was prepared using TRIzol reagent (Invitrogen Life Technologies) according to the manufacturer's protocol. Reverse transcription was done with the ThermoSCRIPT reverse transcription–PCR system (Invitrogen Life Technologies), according to the manufacturer's protocol. A total RNA of 1 μg was used for the first strand cDNA synthesis using oligo (dT) 15 primer. The complete coding region of hHSG was amplified from human tumor cells cDNA library by PCR using the forward primer 5′-ATGTCCCTGCTCTTCTCTCGATGC-3′ and reverse primer 5′-TCTGCTGGGCTGCAGGTACTGGT-3′. The PCR reaction for hHSG amplification was carried out with one cycle of 94°C for 5 min and 30 cycles of 94°C for 1 min, 60°C for 1 min, 72°C for 2 min, followed by a one cycle extension at 72°C for 7 min. For glyceraldehyde-3-phosphate dehydrogenase (internal control) primers, forward primer 5′-CCACCCATGGCAAATTCCATGGCA-3′, reverse primer 5′-TCTAGACGGCAGGTCAGGTCAGGTCCACC- 3′ were used, and PCR reaction was done at an annealing temperature of 58°C for 20 cycles. PCR products were separated via 1.0% agarose gel electrophoresis and visualized by ethidium bromide staining.

Protein Extraction and Immunoblotting

The level of hHSG protein expression, the release of cytochrome *c*, and cleavage of PARP were examined by immunoblotting technique. Cells were extracted using a lysis buffer (10 mmol/L HEPES, 150 mmol/L NaCl, 1 mmol/L EDTA, 1 mmol/L EGTA, 1% Triton-X100, 0.5% NP40, 0.1% SDS, and with freshly added proteinase inhibitor cocktail) for 30 min on ice. The protein concentration was quantified using the bicinchoninic acid protein assay reagent (Pierce). Equal amounts of protein (30 μg) were separated by SDS-PAGE and transferred onto nitrocellulose membranes (Amersham Pharmacia). Membranes were incubated overnight at 4°C with the appropriate primary antibodies (anti-HSG rabbit polyclonal antibody, 1:1,000, bestowed by Shigehisa Hirose, Department of Biological Sciences, Tokyo Institute of Technology; anti–cytochrome *c* mouse monoclonal antibody, 1:1,000, BD PharMingen; anti-PARP rabbit polyclonal antibody, 1:1,000, Cell Signaling Technology; anti-Bax rabbit polyclonal antibody, 1:1,000, Abcam). Incubated for 1 h in the dark with the appropriate IRDye 800–conjugated secondary antibodies (1:5,000, LI-COR Bioscience, Inc.), the signals were detected using the Odyssey Imaging System (LI-COR Bioscience, Inc.).

For immunoblotting of cytosolic cytochrome *c*, cells were harvested, washed, and resuspended in 0.2 mL lysis buffer [250 mmol/L sucrose, 20 mmol/L HEPES (pH 7.5), 0.1 mmol/L EDTA, 0.1% fatty acid–free bovine serum albumin with proteinase inhibitor cocktail freshly added]. Cell suspensions were gently homogenized with a Dounce Homogenizer, and the homogenates were centrifuged (2,000 rpm, 15 min, 4°C). Supernatants were then centrifuged (12,000 rpm, 30 min, 4°C), after which the supernatants were used for identification of cytosolic cytochrome *c* by immunoblotting.

Confocal Microscopy and Electron Microscopy

To visualize the mitochondrial fusion, the live A549 and HT-29 cells infected without or with Ad5-hHSG at 25, 50, 100 MOI were stained with MitoTracker Red CMXRos (150 nmol/L; Molecular Probes) and observed by confocal laser scanning microscopy (Leica TCS SP2, Leica Microsystems AG). For electron microscopy, the indicated cells were initially fixed in 0.01 mol/L sodium phosphate buffer containing 2.5% glutaraldehyde (pH 7.4). Next, cells were fixed, dehydrated, embedded, and sliced as described by Wang et al. (11). Ultrathin sections were stained with uranyl acetate and lead citrate and examined with a JEM-1230 transmission electron microscope (JEOL).

Flow Cytometry Analysis of Apoptosis

A549 and HT-29 cells were seeded in 60-mm dishes in DMEM plus 10% fetal bovine serum. After 12 h, medium was changed in DMEM plus 5% fetal bovine serum without (mock) or with Ad5-Null or Ad5-hHSG. Cells were collected at 24, 48, and 72 h and first stained with FITC-conjugated Annexin V for 30 min at room temperature and then stained with propidium iodide before 1 min analyzed by FACScan. Annexin V and propidium iodide were added according to the manufacturer's

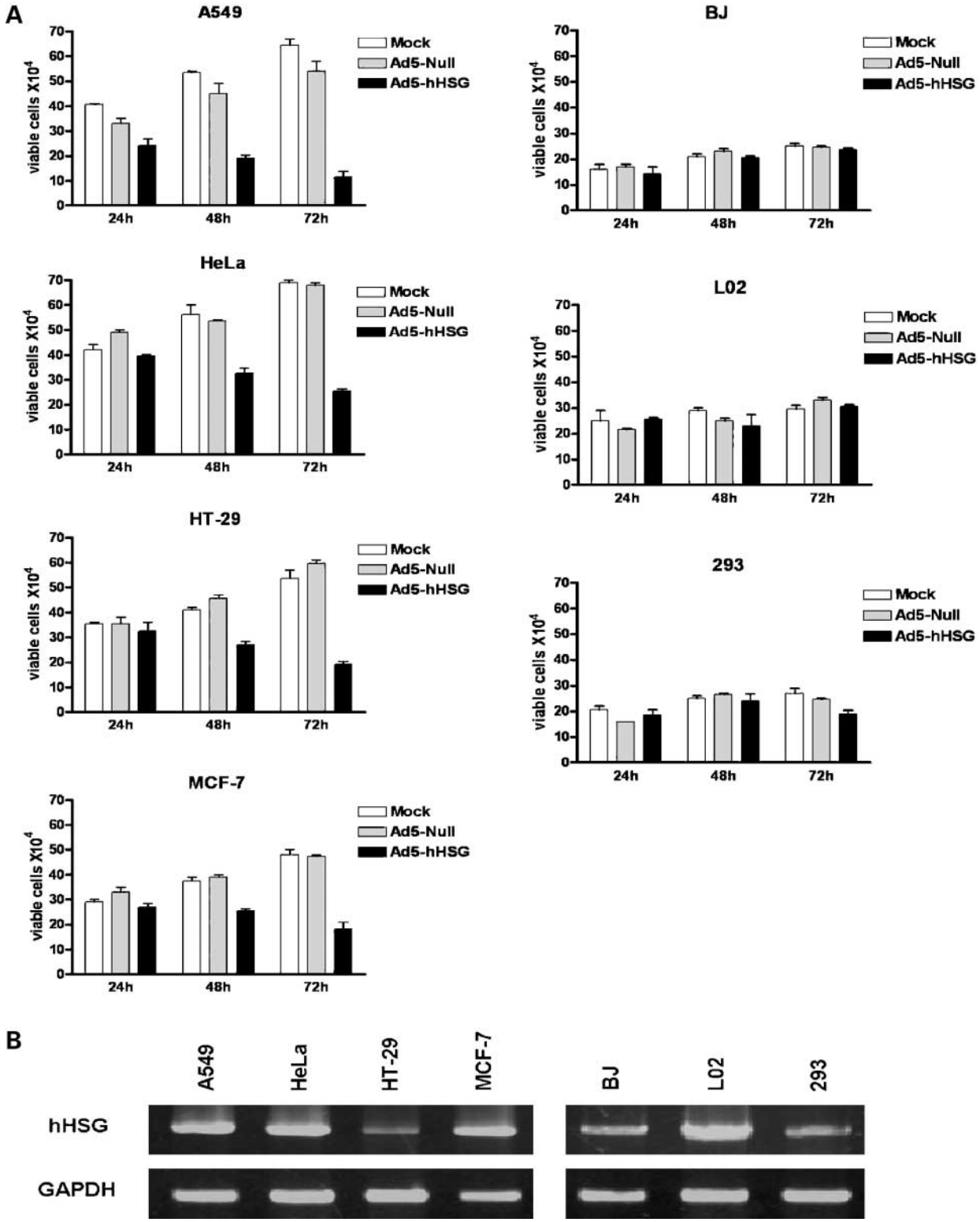

Figure 1. Effect of Ad5-hHSG and endogenous hHSG expression at mRNA level in four cancer and three diploid cell lines. **A,** the indicated cells, including four cancer cell lines A549, HT-29, HeLa, and MCF-7 and three diploid cell lines BJ, L02, and 293, were uninfected (mock) or infected with 100 MOI of Ad5-Null or Ad5-hHSG. Cell viability was analyzed 48 h postinfection using a Vi-CELL XR cell viability analyzer. Columns, mean; bars, SD. **B,** reverse transcription – PCR results for endogenous hHSG mRNA expression. Glyceraldehyde-3-phosphate dehydrogenase (*GAPDH*) was used as an internal control (full-length gels were presented in Supplementary Fig. S1).[3]

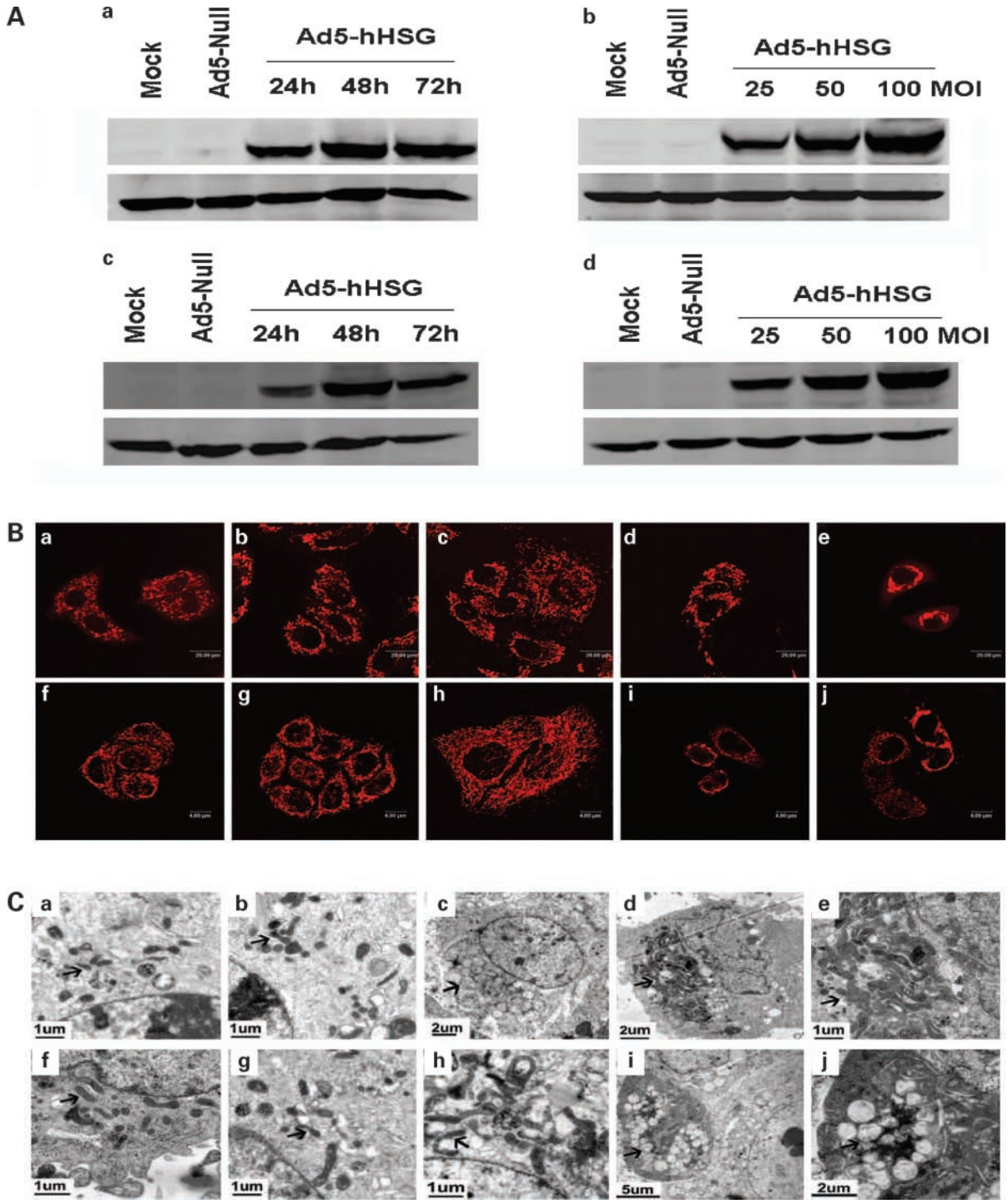

Figure 2. Ad5-hHSG overexpression induced mitochondrial morphologic change. **A,** dose-dependent and time-dependent expression of Ad5-hHSG in A549 and HT-29 by Western blot. hHSG expression 48 h after infection of A549 cells and HT-29 cells with 25, 50, and 100 MOI of Ad5-Null or Ad5-hHSG. hHSG expression after 24, 48, and 72 h treatment of A549 cells and HT-29 cells with 100 MOI Ad5-Null or Ad5-hHSG. β-Actin was used as the protein loading control (full-length blots were presented in Supplementary Fig. S2).[3] **B,** Ad5-hHSG induced mitochondrial aggregation in a dose-dependent manner after 48-h infection of A549 (*a–e*) and HT-29 (*f–j*) cells. Mitochondrial morphologic changes were shown using confocal laser scanning microscopy after staining with MitoTracker Red. *Bars,* 20 μm (*a–e*) and 4 μm (*f–j*). **a, f,** mock; **b, g,** 100 MOI Ad5-Null; **c, h,** 25 MOI Ad5-hHSG; **d, i,** 50 MOI Ad5-hHSG; **e, j,** 100 MOI Ad5-hHSG. **C,** electron microscopic evaluation of Ad5-hHSG–mediated effect on mitochondrial morphology (*arrows*) after 48-h infection with 100 MOI in A549 (*a–e*) and HT-29 (*f–j*). **a, b, f, g,** uniformly spread mitochondria; **d, e, h,** clustered, elongated, tubular mitochondria around nucleus; **c, i, j,** swollen mitochondria clusters. *Bar,* 1 μm (*a,b,e–h*), 2μm (*c, d, j*), and 5 μm (*i*). **a, f,** mock; **b, g,** 100 MOI Ad5-Null; **c–e, h–j,** 100 MOI Ad5-hHSG.

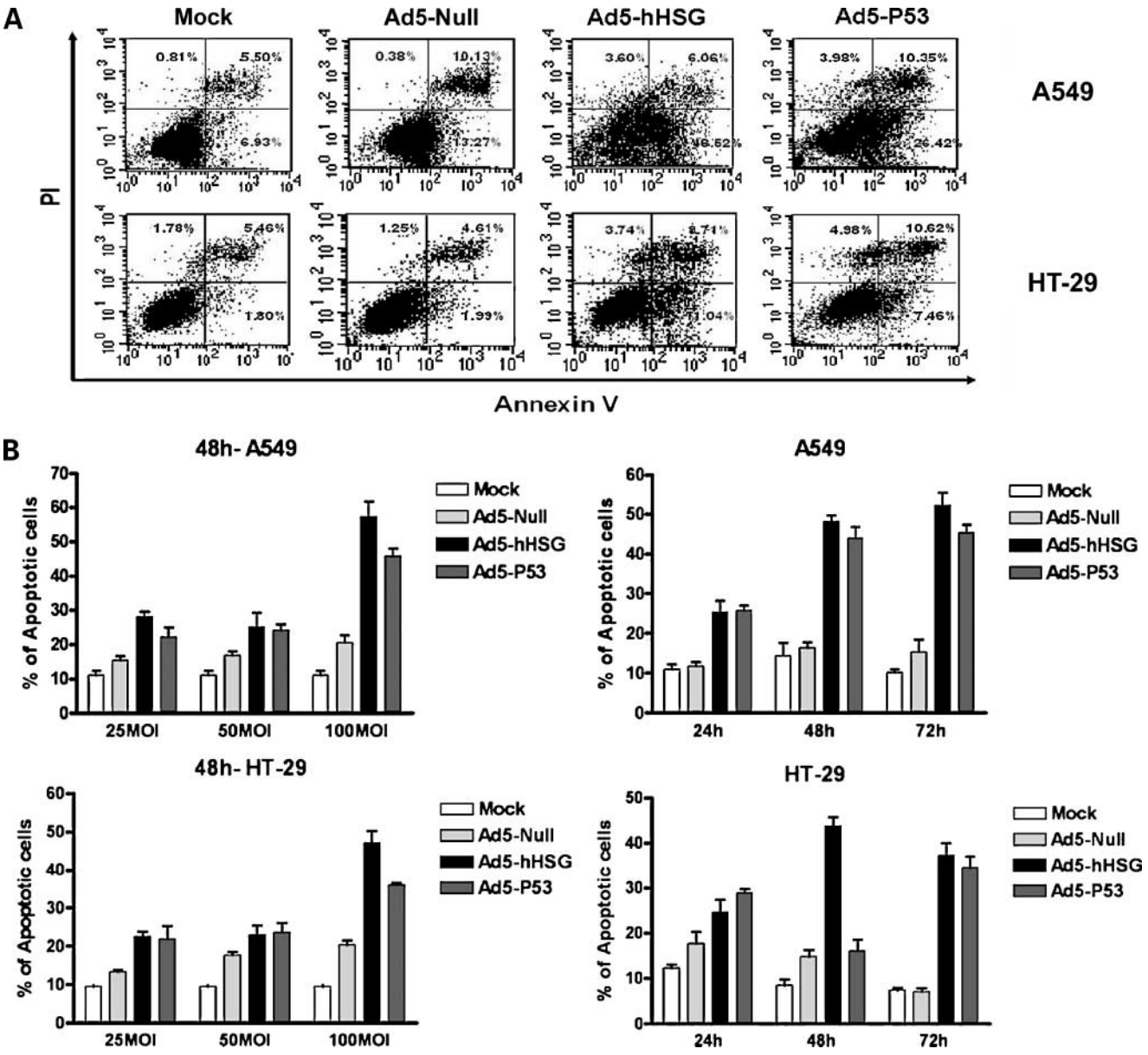

Figure 3. Ad5-hHSG induced cancer cells apoptosis *in vitro*. **A,** apoptotic cells were counted as early or late apoptotic cells (*top* and *bottom right quadrants*) after 48 h infection with mock or 100 MOI of Ad5-Null, Ad5-hHSG, or Ad5-P53. **B,** after 48 h infection with mock or 25, 50, 100 MOI Ad5-Null, Ad5-hHSG, or Ad5-P53, the percentage of apoptotic cells was calculated in A549 and HT-29 cells. After 24, 48, and 72 h with 100 MOI Ad5-hHSG infection, the percentage of apoptotic cells was calculated in A549 and HT-29 cells. Columns, mean; bars, SD.

recommendations (BioVision). Detection and quantification of apoptotic cells was obtained by flow cytometry analysis (Becton Dickinson).

Ex vivo and *In vivo* Treatments with Adenoviruses

All animal experiments were done in accordance with the guidelines of the Institutional Animal Care and Use Committee. Female nu/nu nude mice, 4 weeks of age, were obtained from the Institute of Laboratory Animal Science and kept in a dedicated animal facility with five mice per cage. For *ex vivo* experiment, adenovirus-infected cancer cells were injected into the armpit of BALB/c nude mice in a total volume of 100 μL (5.0×10^6 cells). When the tumors reached 4 mm in diameter, the tumor sizes in two perpendicular diameters were measured with precision calipers everyday. For *in vivo* experiment, 5×10^6 cells were inoculated s.c. into the armpit of BALB/c nude mice. When the tumors reached 5 mm in diameter, 1×10^9 plaque-forming units of Ad5-Null or Ad5-hHSG diluted in 50 μL adenovirus stock solution [4% sucrose, 10 mmol/L Tris (pH 8.0), 2 mmol/L $MgCl_2$] or adenovirus stock solution alone were intratumorally injected thrice (days 5, 10, and 15 for A549; days 5, 8, and 12 for HT-29). Tumor

volume was calculated by using the standard formula: $a \times b^2 \times 0.52$ (a is the longest diameter; b is the shortest diameter). Animals showing severe distress or with tumors that exceeded 15 mm in two perpendicular diameters or 20 mm in one diameter were killed.

Chemosensitization and Radiosensitization Assay

Cells were infected with Ad5-Null and Ad5-hHSG at 100 MOI when adhered. After infection for 12 h, cells were added with VP16 (etoposide, 1 mg/L; Sigma) or CHX (cycloheximide, 1 mg/L; Sigma) for chemotherapy or irradiated with different doses of γ-radiation (0, 4, 8, 12 Gy for A549 and 0, 2, 4, 6 Gy for HT-29) at room temperature for radiotherapy. After 48 h, treated cells were collected and stained with FITC-conjugated Annexin V and propidium iodide to analyze apoptosis as described above.

Measurement of ΔΨm

$DiOC_6(3)$ is used to evaluate whether Ad5-hHSG–induced apoptosis is associated with the disruption of ΔΨm. After 48-h infection without or with adenoviruses at 100 MOI, cells were harvested and incubated with PBS containing 40 μmol/L $DiOC_6(3)$ for 5 min at 37°C. Subsequently, analysis was done with FACSCalibur flow cytometer.

Evaluation of Caspase-3 Activity (DEVDase Activity Analysis)

DEVDase activity analysis is a quantitative method of detecting caspase-3 as described (12). Samples were prepared in triplicate.

Statistical Analysis

Results were expressed as mean ± SD. One-way ANOVA was used for statistical comparison among three groups, and post-hoc test (LSD) was used for statistical comparison between two groups. The differences between groups were considered to be statistically significant when the P value was <0.05.

Results

Ad5-hHSG Has a Wide Antitumor Effect *In vitro*

Firstly, we constructed an adenovirus expression vector of hHSG and examined the role of Ad5-hHSG in cell survival. Cancer cell lines A549, HeLa, HT-29, MCF-7, and normal diploid cell lines BJ, L02, and HEK293 were infected in the absence or presence of 100 MOI of Ad5-Null and Ad5-hHSG. Using cell viability assay, we analyzed the antitumor effect of hHSG at 24, 48, and 72 h, respectively. As time elapsed, Ad5-hHSG overexpression significantly decreased the number of viable cells in all four cancer cell lines compared with diploid cell lines BJ, L02, and 293 (Fig. 1A). We further measured endogenous hHSG mRNA expression in these seven cell lines and found that all the cell lines expressed different levels of hHSG (Fig. 1B). These data indicate that overexpressing hHSG has a wide antitumor effect *in vitro*, whereas it has no effect on diploid cells.

Ad5-hHSG Overexpression Induces Mitochondrial Morphologic Change

To further investigate the antitumor activity of hHSG, we chose two epithelial cancer cell lines, A549 and HT-29, to examine. A549 and HT-29 cells were treated without or with Ad5-hHSG at 25, 50, and 100 MOI for 48 h. Treatment of A549 and HT-29 cells with Ad5-hHSG resulted in a significant dose-dependent overexpression of hHSG as assessed by Western blot (Fig. 2A-a,c). A549 and HT-29 cells were also treated with 100 MOI Ad5-hHSG for 24, 48, and 72 h. Treatment of A549 and HT-29 cells with Ad5-hHSG resulted in a significant time-dependent overexpression of hHSG (Fig. 2A-b,d).

To detect the mitochondrial morphologic change after overexpressing hHSG, confocal and electron microscopy were done. After 48-h infection with 25, 50, or 100 MOI of Ad5-hHSG, mitochondrial morphology was dramatically altered in cells infected with all three MOIs compared with cells treated with Ad5-Null or mock and ranged from conversion of the normal dispersed distribution of punctate mitochondria (Fig. 2B-a,b,f,g) to more reticular structures (Fig. 2B-c,d,h) and to extensive perinuclear clustering (Fig. 2B-e,i,j) by confocal microscopy. This result shows that hHSG overexpression causes mitochondrial fusion and morphologic changes in a dose-dependent manner. In electron microscopy, mitochondria shifted from being uniformly spread (Fig. 2C-a,b,f,g) into forming a complex tubular network (Fig. 2C-d,e,h), even a mass of swollen mitochondria clusters around nucleus at 100 MOI of Ad5-hHSG (Fig. 2C-c,i,j).

Ad5-hHSG Induces Cancer Cells Apoptosis *In vitro*

To determine whether the Ad5-hHSG–mediated decrease in viable cells occurred via apoptosis, A549 and HT-29 cells were analyzed for apoptotic changes by fluorescence-activated cell sorting analysis. After 48 h infection with mock, Ad5-Null, Ad5-hHSG, and Ad5-P53 at 100 MOI, the percentage of apoptotic cells in response to Ad5-hHSG or Ad5-P53 increased by 1.33× and 0.57× over Ad5-Null in A549 cells and 2.14× and 1.74× in HT-29 cells, respectively (Fig. 3A). Ad5-hHSG–induced apoptosis of both cell types occurred in time-dependent and dose-dependent manner. At 24 h, hHSG-induced cancer cell apoptosis was not significantly greater than that of the Ad5-Null–treated controls. At 48 h, Ad5-hHSG or Ad5-P53 treatment resulted in a significant dose-dependent increase in the number of apoptotic cells at both the early and late stages of apoptosis. The percentage increase after Ad5-hHSG infection ranged from 8.21% to 36.68% in A549 cells and from 5.24% to 26.71% in HT-29 cells, which was higher than that induced by Ad5-P53 infection, which ranged from 6.00% to 25.07% in A549 cells and from 5.94% to 15.67% in HT-29 cells, depending on viral titer. No changes were observed in cancer cells treated with Ad5-Null or mock. By 72 h, Ad5-hHSG still induced higher amounts of apoptosis than Ad5-P53 (Fig. 3B).

To further examine the possible inhibitory effect of hHSG on cell cycle progression, we infected A549 and HT-29 cells for 48 h with 25, 50, and 100 MOI Ad5-hHSG and analyzed cell cycle stages by fluorescence-activated cell sorting. The number of A549 cells in G_0-G_1 phase increased significantly from 7.53% at 25 MOI to 14.06% at 50 MOI and to 17.68% at 100 MOI compared with Ad5-Null–treated cells. In infected HT-29 cells, the cell cycle was arrested in G_2-M,

Table 1. Ad5-hHSG mediated inhibition of tumorigenicity *ex vivo* and *in vivo*

A. Effect of Ad5-hHSG on A549 tumor growth *ex vivo*

	Volume of tumor (mean ± SD; mm³)			
	7 d	8 d	9 d	10 d
Mock	34.4 ± 32.8	28.6 ± 14.1	55.4 ± 41.4	39.7 ± 29.2
Ad5-Null	18.3 ± 17.6	15.5 ± 16.4*	25.8 ± 23.8	18.9 ± 14.6
Ad5-hHSG	0.0 ± 0.0†,‡	0.9 ± 3.1†,‡	14.0 ± 25.3†	9.9 ± 20.4†

B. Effect of Ad5-hHSG on HT-29 tumor growth *ex vivo*

	Volume of tumor (mean ± SD; mm³)			
	4 d	6 d	8 d	10 d
Mock	19.4 ± 15.4	34.3 ± 27.3	90.8 ± 83.1	229.8 ± 162.8
Ad5-Null	19.2 ± 15.2	31.1 ± 22.8	92.7 ± 55.9	242.1 ± 134.1
Ad5-hHSG	0.0 ± 0.0†,‡	1.4 ± 4.5†,‡	1.4 ± 4.5†,‡	0.0 ± 0.0†,‡

C. Effect of Ad5-hHSG on A549 tumor growth *in vivo*

	Volume of tumor (mean ± SD; mm³)			
	5 d	7 d	9 d	11 d
Mock	6.5 ± 4.9	29.4 ± 18.8	63.0 ± 47.2	118.3 ± 88.5
Ad5-Null	6.9 ± 5.0	28.2 ± 18.2	101.7 ± 47.5	121.3 ± 72.9
Ad5-hHSG	15.2 ± 14.8	22.0 ± 17.2	23.1 ± 24.9†,‡	49.8 ± 33.5†,‡

D. Effect of Ad5-hHSG on HT-29 tumor growth *in vivo*

	Volume of tumor (mean ± SD; mm³)			
	7 d	8 d	9 d	10 d
Mock	174.1 ± 102.7	323.2 ± 133.3	463.1 ± 210.2	657.5 ± 266.4
Ad5-Null	185.8 ± 142.9	318.3 ± 225.7	403.1 ± 233.6	498.8 ± 238.8
Ad5-hHSG	149.3 ± 116.5	268.9 ± 183.5	330.6 ± 156.9	370.0 ± 155.2†

NOTE: The volumes of tumors represent mean ± SD (n = 10). One-way ANOVA was used for statistical comparison among three groups, and post-hoc test (LSD) was used for statistical comparison between two groups.
*P < 0.05 Ad5-Null versus mock.
†P < 0.05 Ad5-hHSG versus mock.
‡P < 0.05 Ad5-hHSG versus Ad5-Null.

and the percentage increased from 4.51% at 25 MOI to 5.93% at 50 MOI and to 26.66% at 100 MOI compared with Ad5-Null–treated cells. No obvious changes were observed between Ad5-Null–treated and adenovirus stock solution–treated cells (Supplementary Fig. S3).[3]

Ad5-hHSG Mediates Inhibition of Tumorigenicity *Ex vivo* and *In vivo*

We next sought to determine whether exogenous hHSG affected tumorigenicity both *ex vivo* and *in vivo*. Cells were treated with adenovirus stock solution (mock) or with 100 MOI of Ad5-Null and Ad5-hHSG and injected into nude mice 12 h later. Ad5-hHSG–treated tumor cells almost completely suppressed tumor growth *ex vivo*, whereas Ad5-Null–treated and adenovirus stock solution–treated cells resulted in tumor growth (P < 0.05; Table 1A and B).Our results showed that both A549 and HT-29 cells' tumorigenicity was completely inhibited by Ad5-hHSG, indicating that hHSG protein may have therapeutic efficacy. The therapeutic potential of Ad5-hHSG was further examined using an *in vivo* tumor model. Nude mice were inoculated with tumor cells and injected with adenovirus stock solution, Ad5-Null, or Ad5-hHSG after

[3] Supplementary material for this article is available at Molecular Cancer Therapeutics Online (http://mct.aacrjournals.org/).

Table 1. Ad5-hHSG mediated inhibition of tumorigenicity *ex vivo* and *in vivo* (Cont'd)

A. Effect of Ad5-hHSG on A549 tumor growth *ex vivo*

Volume of tumor (mean ± SD; mm^3)				
11 d	12 d	13 d	14 d	15 d
58.5 ± 50.5	92.2 ± 101.5	166.2 ± 168.2	253.9 ± 285.3	294.6 ± 296.9
41.4 ± 40.7	65.1 ± 54.2	15.8 ± 64.4	240.2 ± 128.3	295.5 ± 160.9
25.8 ± 57.2†	13.9 ± 43.1†	13.2 ± 39.2†,‡	13.4 ± 41.1†,‡	15.9 ± 49.3†,‡

B. Effect of Ad5-hHSG on HT-29 tumor growth *ex vivo*

Volume of tumor (mean ± SD; mm^3)			
12 d	14 d	16 d	18 d
228.0 ± 155.6	361.3 ± 199.7	520.0 ± 300.0	892.6 ± 380.4
375.6 ± 227.3†	377.6 ± 212.9	775.2 ± 577.1	953.3 ± 632.4
0.0 ± 0.0†,‡	0.0 ± 0.0†,‡	5.1 ± 12.0†,‡	3.3 ± 10.6†,‡

C. Effect of Ad5-hHSG on A549 tumor growth *in vivo*

Volume of tumor (mean ± SD; mm^3)				
13 d	15 d	17 d	19 d	21 d
243.5 ± 202.4	342.5 ± 303.0	454.2 ± 357.2	568.9 ± 438.6	579.8 ± 456.7
257.5 ± 219.3	302.7 ± 205.9	408.8 ± 230.4	475.3 ± 229.0	566.3 ± 230.6
87.7 ± 51.7†,‡	114.6 ± 78.4†,‡	193.8 ± 153.7†,‡	222.4 ± 162.8†	256.6 ± 278.0†,‡

D. Effect of Ad5-hHSG on HT-29 tumor growth *in vivo*

Volume of tumor (mean ± SD; mm^3)				
11 d	12 d	13 d	14 d	15 d
976.0 ± 450.3	853.5 ± 380.1	842.0 ± 353.4	1025.7 ± 467.3	1093.5 ± 583.6
692.2 ± 286.4	635.7 ± 212.8	661.1 ± 201.1	831.2 ± 246.4	822.4 ± 215.9
525.1 ± 254.7†	493.3 ± 163.7†	495.9 ± 198.8†	482.6 ± 150.5†,‡	541.1 ± 191.7†

tumorigenesis. Tumor growth was significantly inhibited after Ad5-hHSG treatment from 9th day in A549 and from 14th day in HT-29 compared with Ad5-Null treatment ($P < 0.05$; Table 1C and D).

Ad5-hHSG Increases Cancer Cell Chemosensitization and Radiosensitization

To examine the effect of Ad5-hHSG on chemotheraphy and radiotherapy, chemosensitization and radiosensitization experiments were done. We began by evaluating the antitumor effect of Ad5-hHSG on A549 and HT-29 cells when used in combination with chemotherapy *in vitro* and measuring apoptosis by fluorescence-activated cell sorting. The chemotherapeutic agents VP16 and CHX were used in the combination experiments. Ad5-hHSG and VP16 combination therapy resulted in 47.19 ± 1.76% apoptosis in A549 cells, which was higher than VP16 (14.37 ± 2.14%) or Ad5-hHSG alone (24.18 ± 2.83%). Ad5-P53 and VP16 combination therapy only reached 29.72 ± 3.87%, although this was higher than single treatment with Ad5-P53 (24.53 ± 2.06%) or VP16 (14.37 ± 2.14%). Ad5-P53 also had a synergistic effect on CHX sensitization (23.76 ± 2.81%) in A549 cells; however, Ad5-hHSG had an even stronger effect (42.23 ± 2.91%; Fig. 4A). Ad5-hHSG also significantly increased the VP16 (40.15 ± 4.21%) and CHX (32.93 ± 1.99%) sensitivity of HT-29 cells and had a greater effect than Ad5-P53 and VP16 (27.41 ± 5.56%) or CHX (21.15 ± 3.40%; Fig. 4B).

We also observed the combining effect of Ad5-hHSG and radiotherapy. Ad5-hHSG treatment of A549 cells only produced modest tumor cell apoptosis (21.31 ± 2.82%), whereas treatment with γ-radiation increased apoptosis from 17.81 ± 0.66% to 33.64 ± 1.95%. Combination therapy with Ad5-hHSG and radiation resulted in between 38.64 ± 1.93% and 48.95 ± 0.97% apoptosis, which was slightly

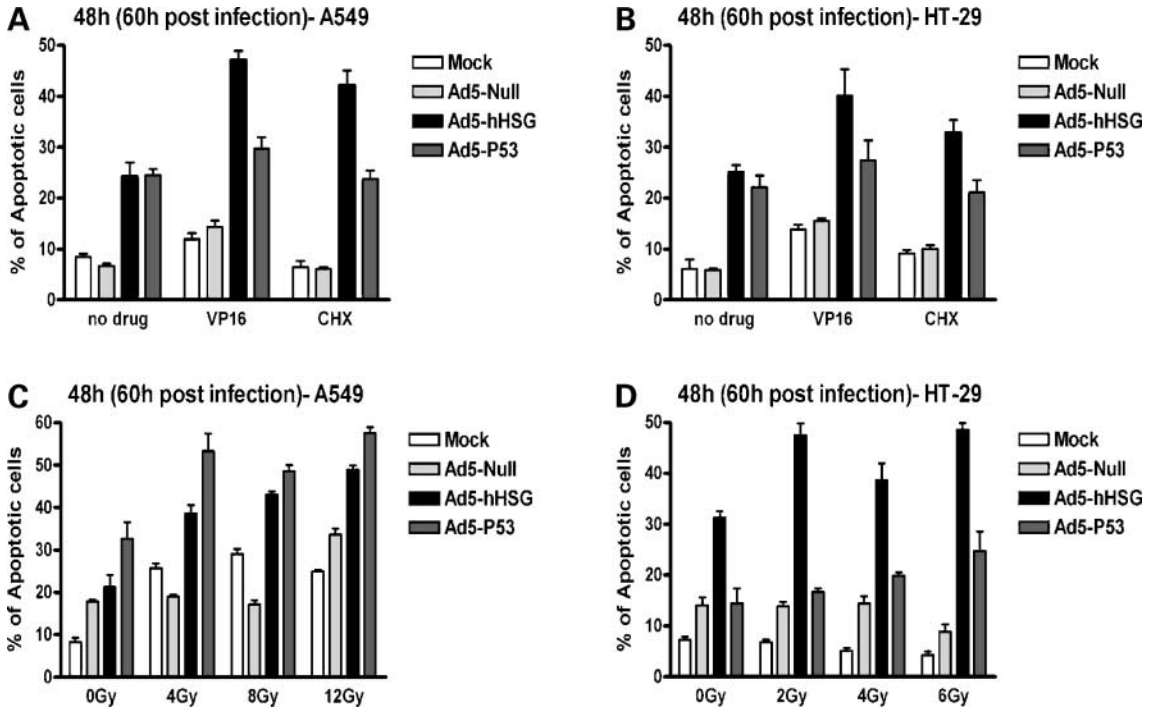

Figure 4. Ad5-hHSG increased the chemosensitization and radiosensitization of tumor cells. After 12 h infection with mock or 100 MOI of Ad5-Null, Ad5-hHSG, or Ad5-P53, respectively, cells were chemosensitized with VP16 (1 mg/L) or CHX (1 mg/L) or irradiated with different doses (0, 4, 8, and 12 Gy for A549 cells and 0, 2, 4, and 6 Gy for HT-29 cells) at room temperature. Cells were collected at 48 h, and apoptotic cell numbers were quantitated by fluorescence-activated cell sorting. **A** and **B,** Ad5-hHSG in combination with chemotherapeutic agents enhanced apoptosis in A549 and HT-29 cells. **C** and **D,** Ad5-hHSG combined with radiation therapy enhanced A549 and HT-29 cell apoptosis. Columns, mean; bars, SD.

lower than Ad5-P53 and radiation combination treatment (between 48.59 ± 2.07% and 57.55 ± 2.07%; Fig. 4C). In HT-29 cells, Ad5-hHSG and radiation treatment ranged from 38.67 ± 3.30% to 48.61 ± 1.28% and was higher than radiation and Ad5-P53 treatment, which ranged from 16.65 ± 1.06% to 24.73 ± 5.36% (Fig. 4D). Because the synergic antitumor activity of Ad5-hHSG is independent of the state of endogenous hHSG, this makes it a better agent than Ad5-P53.

High-Dose Ad5-hHSG Induces ΔΨm Reduction and Release of Cytochrome *c*

To evaluate whether the apoptotic effect of hHSG is associated with the mitochondrial apoptotic pathway, ΔΨm was measured. Loss of ΔΨm was visualized as a reduction in the fluorescence signal in the FL1 channel. Infection of A549 and HT-29 cells with 100 MOI of Ad5-hHSG for 48 h reduced ΔΨm. The percentage of negative fluorescence induced by Ad5-hHSG in A549 cells was 26.55% compared with 10.40% and 6.28% induced by mock and Ad5-Null, respectively. Ad5-hHSG induced 13.00% in HT-29 cells compared with 6.22% and 5.08% induced by mock and Ad5-Null, respectively (Fig. 5A). Involvement of the mitochondrial apoptotic pathway was confirmed by the release of cytochrome *c* from mitochondria to cytosol after infection (Fig. 5B). We also analyzed caspase-3 activity in infected cells using DEVDase activity analysis (13) and Western blot. At 48 h postinfection with 100 MOI, DEVD cleavage in lysates from hHSG-infected A549 cells was at least four times higher than from mock or Ad5-Null–infected cell lysates. hHSG infection of HT-29 cells resulted in 21.8× higher DEVD cleavage (Fig. 5C). PARP, as a representative substrate of caspase-3, was cleaved in Ad5-hHSG–infected cells (Fig. 5D).

Discussion

In this study, we firstly confirmed the antitumor activity of Ad5-hHSG in a wide range of cancer cell lines. Using adenovirus-expressed hHSG, we found that it significantly affected the survival of different epithelial cancer cell lines. However, it was not efficient in some diploid cell lines, suggesting that its effect on cell survival has a tendency toward cancer cells. It still remains unknown why normal cells are insensitive to Ad5-hHSG. To investigate the antitumor activity of Ad5-hHSG and its mechanism, we selected two cancer cell lines, A549 and HT-29, and did a series of experiments. Ad5-hHSG could induce mitochondrial perinuclear clustering, trigger apoptosis, arrest cell cycle, decrease the ΔΨm, and subsequently release cytochrome *c* in both cancer cell lines. In an animal model, the tumorigenicity of A549 and HT-29 was significantly inhibited by Ad5-hHSG treatment. The antitumor activity of Ad5-hHSG is independent of the

state of endogenous hHSG, making it even more effective than P53. In addition, Ad5-hHSG significantly increased the sensitivity of cancer cell lines to chemotherapeutic agents and γ-radiation.

rHSG (*rMfn2*) is a powerful regulator of cell proliferation both *in vitro* and *in vivo* (1). Overexpression of rHSG with the adenovirus vector Ad5-rHSG inhibited mitogenic stimuli–mediated proliferation of cultured Wistar-Kyoto vascular smooth muscle cells and blocked balloon injury induced by neointimal vascular smooth muscle cell proliferation and restenosis *in vivo*. However, when Mfn2 was overexpressed using eukaryotic expression vectors, Mfn2 and its variant, Mfn2RasG12V (''activated Mfn2''), inhibited Bax activation, release of cytochrome *c*, and cell death (14–16). These results contrast with our current findings. Why would the same gene have a different effect in different laboratories? One possibility is that adenovirus expression vectors allow for higher expression level of hHSG than plasmid expression vectors. Before this study, we compared hHSG expression using plasmid and adenovirus vectors and found that expression levels were much lower with the plasmid vector and there was no apoptosis although mitochondrial fusion was also observed (Supplementary Fig. S5).[3] When the eukaryotic expression plasmid containing hHSG was over highly expressed, we could detect cell growth inhibition and few cancer cells undergoing apoptosis (17). With the adenovirus vector Ad5-hHSG, mitochondrial perinuclear clustering appeared at 25 MOI, whereas swollen mitochondrial clusters and extensive cancer cell apoptosis were observed as the dose increased to 100 MOI. Our results suggest that Ad5-hHSG–mediated overexpression significantly elevated cancer cell apoptosis.

The antitumor mechanism of hHSG remains unclear. We first supposed that hHSG might be involved in cancer based on its location on chromosome 1p36.3. Cytogenetic analysis of various types of human malignancies, ranging from solid tumors to leukemias and myeloproliferative disorders, have shown nonrandom involvement of abnormalities on chromosome 1p36 (18, 19). In the past few decades, many tumor suppressor genes have been found in this region (20, 21). In our preliminary study, we detected endogenous hHSG in both normal and cancerous tissue by immunohistochemistry and *in situ* hybridization; however, the positive rate of hHSG was lower in cancer (51.51%) than normal tissue (68.96%; data not shown). Down-regulated expression or loss-of-function of hHSG in cancers might have a role in the development of cancers.

In addition, as a mitochondrial dynamic protein, hHSG overexpression has an effect on mitochondrial morphology and functions. Our findings show that hHSG induced cancer cell apoptosis, along with ΔΨm reduction and release of cytochrome *c*, assuming that Ad5-hHSG–induced apoptosis is associated with Bax. Bax is a member of the Bcl-2 family of proteins known to regulate mitochondria-dependent programmed cell death (22, 23). Early in apoptosis, Bax translocates from the cytosol to the mitochondrial membrane. Then Bax leaves the mitochondrial membranes and coalesces into large clusters containing thousands of Bax molecules that remain adjacent to mitochondria (24). Bax proapoptotic mechanism is immediately subsequent to mitochondrial translocation. It has

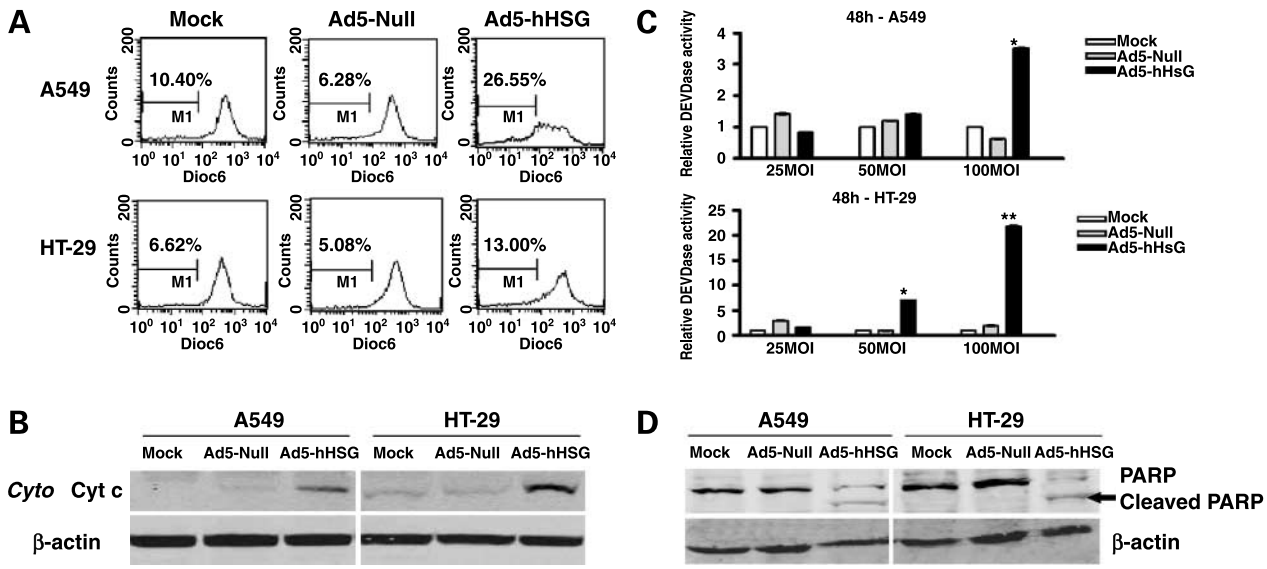

Figure 5. Ad5-hHSG induced ΔΨm reduction and release of cytochrome *c*. **A,** ΔΨm as reflected by $DiOC_6(3)$ staining of infected cells was determined at 48 h after infection. The proportions of cells with reduced $DiOC_6(3)$ staining. The results depicted were a representative of three independent experiments. **B,** Western blotting for the release of cytochrome *c* from mitochondria to cytosol 48 h after infection. β-Actin was used as the protein loading control. **C,** DEVDase activity assay. Cell lysates were extracted after 48-h infection. Columns, mean ($n = 3$); bars, SD. Significant difference from mock-transfected cells: *, $P < 0.05$; **, $P < 0.001$. **D,** Western blotting for cleavage of PARP 48 h after infection. β-Actin was used as the protein loading control (full-length blots were presented in Supplementary Fig. S4).[3]

been proposed that Bax interacts with the coiled-coil domain of hHSG (Mfn2) to induce mitochondrial fusion (8). However, in our experiments, after we silenced endogenous Bax expression using small interfering RNA, the apoptotic inhibitory rate of siBax group was only approximately 20% compared with nonsilencing group (Supplementary Fig. S6A,B).[3] Our results suggested that siBax could partly inhibit Ad5-hHSG-induced apoptosis. Also, we found that silencing endogenous Bax prevented the release of cytochrome *c* to cytosol, but it did not affect the cleavage of PARP (which is a substrate of caspase-3). As is known to us, caspase-3, a key factor in apoptosis execution, participates in mitochondrial and nonmitochondrial apoptotic pathway. These results further proved that Ad5-hHSG–induced apoptosis was via both Bax-dependent mitochondrial apoptotic pathway and Bax-independent apoptotic pathway. Another possibility is that Ad5-hHSG–induced mitochondrial excessive fusion directly leads to the irreversible pathologic changes of mitochondrial morphology and induces apoptosis.

At present, multiple therapies are used to treat cancers. Intratumoral injection of Ad-P53 (INGN201) in combination with radiation therapy is well tolerated and shows evidence of primary injected tumor regression (25). Exogenous overexpression of P53 in combination with DNA-damaging agents may increase susceptibility to apoptosis specifically by tumor cells (26). Our previous study suggests that hHSG inhibits tumor cell proliferation and increases their sensitivity to chemotherapy (17). In this study, we are excited to find that Ad5-hHSG increased the radiosensitization and chemosensitization of A549 and HT-29 cells even above Ad5-P53. Although additional *in vivo* experiments are needed, the knowledge that Ad5-hHSG sensitizes A549 and HT-29 cells to VP16, CHX, and radiation may provide a foundation for new therapeutic approaches.

In summary, howbeit hHSG is a gene participating in mitochondrial fusion and overexpression of Ad5-hHSG has a strong antitumor activity *in vitro* and *in vivo* and sensitizes cells to chemotherapy and radiation therapy more effectively than Ad5-P53. Our present data indicate that Ad5-hHSG is a potential gene therapeutic drug.

Acknowledgments

We thank Shigehisa Hirose for the anti-HSG rabbit polyclonal antibody, Prof. Zhiqian Zhang and Lan Yuan for help with confocal laser scanning microscope.
This manuscript was proofread by an English speaking professional with science background at Elixigen Corporation.

References

1. Chen KH, Guo X, Ma D, et al. Dysregulation of HSG triggers vascular proliferative disorders. Nat Cell Biol 2004;6:872 – 83.

2. Chen G, Zhang C, Zhu Y. [Cloning and expression of a novel gene related to hypertension]. Zhonghua Yi Xue Za Zhi 1997;77:823 – 8.

3. Chen G, Liu N, Zhou A, Tang C, Ma D, Tang J. The role of hypertension-related gene in aortic vascular smooth muscle cells from mice and rats. Chin Med J (Engl) 2001;114:833 – 6.

4. Hales KG, Fuller MT. Developmentally regulated mitochondrial fusion mediated by a conserved, novel, predicted GTPase. Cell 1997; 90:121 – 9.

5. Santel A, Fuller MT. Control of mitochondrial morphology by a human mitofusin. J Cell Sci 2001;114:867 – 74.

6. Rojo M, Legros F, Chateau D, Lombes A. Membrane topology and mitochondrial targeting of mitofusins, ubiquitous mammalian homologs of the transmembrane GTPase Fzo. J Cell Sci 2002;115:1663 – 74.

7. Chen H, Detmer SA, Ewald AJ, Griffin EE, Fraser SE, Chan DC. Mitofusins Mfn1 and Mfn2 coordinately regulate mitochondrial fusion and are essential for embryonic development. J Cell Biol 2003;160: 189 – 200.

8. Karbowski M, Norris KL, Cleland MM, Jeong SY, Youle RJ. Role of Bax and Bak in mitochondrial morphogenesis. Nature 2006;443:658 – 62.

9. Karbowski M, Lee YJ, Gaume B, et al. Spatial and temporal association of Bax with mitochondrial fission sites, Drp1, and Mfn2 during apoptosis. J Cell Biol 2002;159:931 – 8.

10. He TC, Zhou S, da Costa LT, Yu J, Kinzler KW, Vogelstein B. A simplified system for generating recombinant adenoviruses. Proc Natl Acad Sci U S A 1998;95:2509 – 14.

11. Wang L, Yu C, Lu Y, et al. TMEM166, a novel transmembrane protein, regulates cell autophagy and apoptosis. Apoptosis 2007;12:1489 – 502.

12. Lv B, Shi T, Wang X, et al. Overexpression of the novel human gene, nuclear apoptosis-inducing factor 1, induces apoptosis. Int J Biochem Cell Biol 2006;38:671 – 83.

13. Rehm M, Dussmann H, Janicke RU, Tavare JM, Kogel D, Prehn JH. Single-cell fluorescence resonance energy transfer analysis shows that caspase activation during apoptosis is a rapid process. Role of caspase-3. J Biol Chem 2002;277:24506 – 14.

14. Nakamura N, Kimura Y, Tokuda M, Honda S, Hirose S. MARCH-V is a novel mitofusin 2- and Drp1-binding protein able to change mitochondrial morphology. EMBO Rep 2006;7:1019 – 22.

15. Neuspiel M, Zunino R, Gangaraju S, Rippstein P, McBride H. Activated mitofusin 2 signals mitochondrial fusion, interferes with Bax activation, and reduces susceptibility to radical induced depolarization. J Biol Chem 2005;280:25060 – 70.

16. Sugioka R, Shimizu S, Tsujimoto Y. Fzo1, a protein involved in mitochondrial fusion, inhibits apoptosis. J Biol Chem 2004;279:52726 – 34.

17. Wang P, Wu LN, Jiang CS, et al. [Human hyperplasic suppress gene (hHSG) could increase the chemotherapy sensitivity of human tumor cells *in vitro*]. Beijing Da Xue Xue Bao 2005;37:117 – 20.

18. Atkin NB. Chromosome 1 aberrations in cancer. Cancer Genet Cytogenet 1986;21:279 – 85.

19. Weith A, Brodeur GM, Bruns GA, et al. Report of the second international workshop on human chromosome 1 mapping 1995. Cytogenet Cell Genet 1996;72:114 – 44.

20. Mori N, Morosetti R, Spira S, et al. Chromosome band 1p36 contains a putative tumor suppressor gene important in the evolution of chronic myelocytic leukemia. Blood 1998;92:3405 – 9.

21. Smedley D, Sidhar S, Birdsall S, et al. Characterization of chromosome 1 abnormalities in malignant melanomas. Genes Chromosomes Cancer 2000;28:121 – 5.

22. Gross A, McDonnell JM, Korsmeyer SJ. BCL-2 family members and the mitochondria in apoptosis. Genes Dev 1999;13:1899 – 911.

23. Wei MC, Zong WX, Cheng EH, et al. Proapoptotic BAX and BAK: a requisite gateway to mitochondrial dysfunction and death. Science 2001; 292:727 – 30.

24. Nechushtan A, Smith CL, Lamensdorf I, Yoon SH, Youle RJ. Bax and Bak coalesce into novel mitochondria-associated clusters during apoptosis. J Cell Biol 2001;153:1265 – 76.

25. Swisher SG, Roth JA, Komaki R, et al. Induction of p53-regulated genes and tumor regression in lung cancer patients after intratumoral delivery of adenoviral p53 (INGN 201) and radiation therapy. Clin Cancer Res 2003;9:93 – 101.

26. Horio Y, Hasegawa Y, Sekido Y, Takahashi M, Roth JA, Shimokata K. Synergistic effects of adenovirus expressing wild-type p53 on chemosensitivity of non-small cell lung cancer cells. Cancer Gene Ther 2000;7: 537 – 44.

Molecular Cancer Therapeutics

Adenovirus-expressed human hyperplasia suppressor gene induces apoptosis in cancer cells

Lina Wu, Zhixin Li, Yingmei Zhang, et al.

Mol Cancer Ther 2008;7:222-232.